Deforestation in North-Central Yucatan (1985-1995): Mapping Secondary Succession of Forest and Agricultural Land Use in Sotuta Using the Cosine of the Angle Concept

Youngsinn Sohn, Emilio Moran, and Francisco Gurri

Abstract

A new spectral pattern matching approach that utilizes the spectral angle (the cosine of the angle) concept was used for mapping deforestation and successional stages of forest regrowth in Sotuta in the state of Yucatan, Mexico. By calculating spectral angles between finely defined spectral clusters and known reference signatures, and assigning each spectral cluster to one of the reference classes based on the minimum spectral angle rule, we were able to map forest regrowth stages and agricultural land-use classes. Our research shows that, by adapting a spectral pattern matching approach demonstrated in this paper, spectral clusters can be assigned into information classes precisely and objectively, and the inconsistency involved in visual interpretations can be avoided. The conceptual difference between the spectral distance and spectral angle in feature space is also reviewed.

In the study area, the rate of deforestation is high and agricultural land use is intensifying increasingly. The limited amount of land granted to ejidos *and rapid population growth seem to be major causes of deforestation in the study area.*

Introduction

Since the Mexican revolution, Mayans have cultivated communal lands, or *ejidos*, granted to them. These *ejidos* are sections of land managed and governed communally by each community. The head of each family within the community is entitled to a certain amount of land. In the state of Yucatan, an average *ejidatario*, a peasant with *ejido* land rights, is entitled to 24 to 35 hectares. In the maize region of Yucatan, an average family cultivates three hectares of newly cleared land and one hectare of second-year *milpa* (maize) per agricultural cycle (Duch, 1992). While the institution of *ejido* guarantees peasant communities their land rights, the boundaries of *ejido*, however, limit the necessary mobility of practicing slash and burn shifting agriculture. *Ejidatarios* are allowed to practice slash and burn shifting agriculture only within the boundaries of the allotted *ejido*. This was not viewed as an immediate problem when *ejidos* were granted. Since then, natural population increase, in-migration, and the introduction of cattle onto plots that could have been rented by the peasants have limited the available land for slash and burn shifting agriculture (Duch, 1992; Ku, 1992). In 1993, the Mexican Congress approved an initiative by president Carlos Salinas de Gortarí, to amend Article 27 of the Mexican constitution permitting the privatization of *ejido* lands. *Ejidos* may now be bought, sold, mortgaged, and subdivided. *Ejido* communities may now enter into business agreements with local and foreign investors. The impacts of this change on *eijdo* communities remain to be seen.

In recent years, deforestation and decline in maize production in Yucatan have been reported by several researchers (Chemas and Rico-Gray, 1991; Duch, 1992; Gates, 1993; Re Cruz, 1996), suggesting that the traditional *milpa* (cornfield) system is under increasing stress of disintegration from socioeconomic and ecological factors (Gates, 1993). Rapid population growth, shortened fallow periods and resulting soil fertility decline, and changes in precipitation pattern are reported as major factors contributing to the current crisis in the traditional *milpa* system (Gates, 1993). Agricultural policies and agricultural development projects that encourage the commercialization of agricultural production and adaptation of new agricultural technologies are also reported as contributing factors causing stress (Gates, 1993; Munguia, 1994). Although deforestation and increasing stress on the traditional *milpa* system have been reported, agricultural land-use changes, the actual rates of deforestation and forest regrowth have not been mapped or estimated in the study area. This study is the first part of a project that involves mapping deforestation and agricultural land-use change in Yucatan, Mexico and assessing the impact of agricultural policy changes on deforestation and the intensity of agricultural land use.

The objectives of this paper are (1) to map deforestation, successional stages of forest regrowth, and agricultural land-

Y. Sohn was with the Anthropological Center for Training and Research on Global Environmental Change (ACT), University of Arizona, Tucson, AZ 85721; she is presently with the Department of Anthropology, Geography and Earth Science, Clarion University of Pennsylvania, Clarion, PA 16214 (ysohn@clarion.edu).

E. Moran was with the Department of Anthropology/ACT, University of Arizona, Tuscon, AZ 85721; he is presently with the Department of Anthropology/ACT, Indiana University, Bloomington, IN 47405.

F. Gurri was with the Department of Anthropology, Indiana University, Bloomington, IN 47408; he is presently with the Division de Salud y Poblacion, Colegio de la Frontera Sur, Carretera Panamericana y Periferico Sur, 29290, San Cristobal de las Casis s/n, Chiapas, A.P. 63 Mexico.

Photogrammetric Engineering & Remote Sensing,
Vol. 65, No. 8, August 1999, pp. 947–958.

0099-1112/99/6508–947$3.00/0

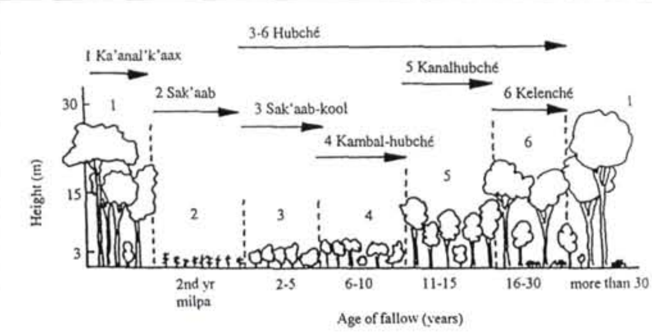

Figure 1. Six stages of Mayan forest succession nomenclature. Reproduced from Gomez-Pompa (1987) in Mexican Studies/Estudios Mexicanos. Copyright © by Regents of the University of California.

use changes in the study area between 1985 and 1995 using Landsat Thematic Mapper (TM) data; and (2) to demonstrate a land-cover mapping approach that utilizes a spectral-pattern-matching method based on the concept of spectral angle (the cosine of the angle).

Study Area

Sotuta is located in the heart of the maize region in the state of Yucatan. The study area includes the *municipio* of Sotuta and adjacent towns, and is roughly 42 km by 30 km of flat limestone lowland. In the study area, there are no perennial streams or channeled surface watercourses. Groundwater erodes the limestone bedrock and creates caves and *cenotes*, natural wells formed by the collapse of the limestone caverns. These caves and *cenotes* are the primary water sources for Mayans. The soil in the study area is thin and rocky. The temperatures are uniform and mild year round. In 1993 the average maximum temperature was 35.2°C and the average minimum temperature was 12.0°C in Sotuta. Precipitation is irregular and highly variable in timing, quantity, and spatial distribution. One *milpa* plot may receive rain while another adjacent plot remains dry (Re Cruz, 1996). The annual precipitation between 1985 and 1995 in Sotuta-Cantamayec area ranges from 1,877mm (1988, Sotuta) to 498mm (1986, Cantamayec). In the study area, maize production is the predominant traditional activity. Beekeeping and cattle-raising are also important economic activities. In the northwest part of the study area near Huhi, henequen (sisal) production has been predominant for more than a century. However, in recent years, most of the henequen fields have been abandoned due to falling prices and the decrease of world demand (Baños Ramírez, 1992; Villanueva, 1993). Some of *ejidatarios* who used to work for henequen plantations have returned to plant their *milpas*.

Shifting Agriculture and Forest Management

Agricultural Cycle

The wet-dry seasonal cycle dictates the maize production cycle. The rainy season starts in May and continues until October. The rainy season is interrupted by a short drought, *la canicula*, from mid-July to mid-August, followed by hurricanes and tropical storms in September and October. In October precipitation decreases drastically and the dry season starts and stays until May. Corn is planted in late May and early June, depending upon the first rain that brings water to *milpas*, and grows in the field until October. The green corn is harvested to be consumed fresh during the growing season. When the dry season starts in October the maize stalks are folded over and the ears of corn are left to dry in the fields. The dried corn is harvested in December (Gates, 1993).

With the harvest of dry corn, the second-year *milpas* that were cultivated in the previous year are abandoned and recovery of forest starts. Around the time of harvest, sometime between October and January, *milperos* look for new lands in the forest to slash trees and burn the fields. The new *milpa* cycle starts with the selection of new locations. The selection of new *milpa* locations is usually based on the proximity of a water supply if possible and on the height and density of the trees, which indicate both the quality of the soil and the age of the fallow. Once a new *milpa* field is chosen, the boundaries of the field are delineated , and the area is measured out in *mecates* (one *mecate* is approximately 20 m by 20 m). The next step is to cut down the trees, preferably very early in the dry season, when the trees are still saturated. For second-year *milpas* that produced crops the previous year, clearing is left to a few weeks before the burn. The burning of fields takes place in April and early May, before the rains begin. The *milpa* will be cultivated for two years and then fallowed (Gates, 1993; Re Cruz, 1996).

Mayan Forest Management

Slash-and-burn shifting agriculture has been practiced for well over two thousand years by Yucatecan Maya in the study area. Traditionally, the Maya managed their forest ecosystems efficiently using very sophisticated silviculture methods and techniques. Maya succession nomenclature (Figure 1) consist of six stages (Gomez-Pompa, 1987):

(1) *Ka'anal'k'aax*: Mature tropical forest (more than 30 years old),
(2) *Sak'aab:* Second-year *milpa*,
(3) *Sak'aab-kool*: 2 to 5 years old succession,
(4) *Kambal-hubché*: 6 to 10 years old succession,
(5) *Kanalhubché*: 11 to 15 years old succession, and
(6) *Kelenché*: 16 to 30 years old succession.

All forest regrowth stages younger than 30 years were protected by allowing at least a 30-year fallow period before they cut trees for agriculture (Chemas and Rico-Gray, 1991). Management of their forest ecosystems was based on soil attributes, age of the fallow, species indicators, and the agricultural potentiality of the site based on past yields. In practicing shifting *milpa* cultivation, the useful tree species on the site chosen for cultivation were carefully selected and remained standing as stumps. Selection criteria of useful trees include the rate of growth, potential values of the tree as firewood and its contribution to the recovery of fertility of the fallow soil, medicinal value, hardness of the wood, toxicity of bark and wood, religious reasons, etc., in addition to food values. The trees protected as stumps and which survived fire became a key factor that determines the succession and the future structure of forest when the field was abandoned (Gomez-Pompa, 1987). This selection process was one of the fundamentals of forest ecosystem management by Yucatecan Maya. Besides this fundamental selection technique, Maya preserved their forest ecosystem through *pet kot* and *tolché*. *Pet kot* is a protected forest patch of various sizes for the purpose of concentrating useful plants and allowing forest to reach a mature stage (Gomez-Pompa, 1987; Rico-Gray and Garcia-Franco, 1991). *Tolché* is a special forest belt of different ages, sizes, and forms protected along the roads, *milpas*, and communal land. However, recent studies suggest that these once sustainable agricultural practices in the study area no longer seem sustainable. Although Mayas still utilize some of their old management techniques, it appears that these traditional Mayan shifting agriculture and forest management techniques are giving way to modern, mechanized agricultural methods that are suitable for commercial agriculture. *Milperos* become increasingly dependent on modern agricultural inputs such as new weeding methods, hybrid seed, fertilizer, and pesticide (Gates, 1993). Recent studies also report shortened fallow periods in the study area. According to Duch (1992), the fallow period had been shortened to less than 16 years during the 1920 to 1940 period from the 50 years at the beginning of the century. Today in Yaxcaba, 53 percent of *ejido* land is fallowed for only 6 to 10 years and 47 percent of the land is fallowed for 11 to 15 years (Ku, 1992). Field observations in the study area during the summer of 1995 by our survey team confirmed the shortened fallow periods observed by Ku in 1992.

According to our observation in the summer of 1995, in the study area, mature forest was practically absent. Forests of the study area were mainly patches of various sizes and successional stages. Thirty-year-old forests were a clear exception. Most observed forests were younger than 16 years old. Relatively mature forest patches (reported to be 40 and 100 years old) were located in private ranches that surround the *ejidos* of Yaxcaba and Sotuta.

Methods

Background

Satellite image analysis has been used for mapping deforestation and identification of forest regrowth stages by several researchers (Brondizio *et al.*, 1996; Cohen *et al.*, 1995; Fiorella and Ripple, 1993; Mausel *et al.*, 1993; Moran *et al.*, 1994; Sader *et al.*, 1989; Steininger, 1996). Sader *et al.* (1989) examined the relationship between tropical forest regrowth stages and the normalized difference vegetation index (NDVI). Sader *et al.* (1989) suggested that the NDVI calculated from Landsat TM data were not significantly correlated with forest regrowth stages in Puerto Rico. Steininger (1996) mapped forest regrowth stages in the Amazon using a maximum-likelihood classifier and evaluated the relationships between the tropical secondary forest regrowth and various vegetation indices. Steininger (1996) found that spectral indices of canopy brightness are significantly correlated with forest regrowth stages but the NDVI might not be a reliable measure for forest regrowth identification. According to Steininger (1996), the near-infrared reflectance, the difference index (NIR-Red), Kauth-Thomas greenness, and percent leaf cover all increase over the first 4 years of fallow period, peak from 4 to 8 years, and decrease from 8 to 13 years. The NDVI rapidly rises over the first 4 years and displays no apparent relation to regrowth stages thereafter.

Mausel *et al.* (1993) identified the spectral characteristics of successional stages of forest regrowth in the Amazon, Altamira, State of Pará, Brazil by relating extensive field information and Landsat TM data (excluding band 1). According to Mausel *et al.* (1993) initial secondary succession shows relatively higher spectral response in TM bands 2 and 3, lower spectral response in near IR (TM band 4), and higher spectral response in moisture absorption bands (TM bands 5 and 7) compared to intermediate and advanced secondary successions. The visible (TM bands 2 and 3) spectral response of intermediate secondary succession is similar to initial secondary succession, but it has a higher green/red (TM bands 2/3) ratio. The near IR spectral response of intermediate secondary succession is much higher compared to initial secondary succession. This spectral pattern of intermediate secondary succession reflects the structural characteristics of intermediate secondary succession with its larger young trees with more biomass and plant moisture compared to initial secondary succession. Advanced secondary succession, with its developing multicanopy structure and increased plant moisture content, generally shows lower spectral response in visible and moisture absorption bands compared to initial and intermediate secondary successions. The near IR spectral response is somewhat lower compared to intermediate secondary succession, but is higher compared to initial secondary succession.

Fiorella and Ripple (1993) mapped successional stages of temperate coniferous forests in the central Cascade Range of Oregon. Fiorella and Ripple (1993) generated 99 spectral clusters using the ISODATA classifier and used ancillary data that include the locations of oldgrowth and mature forest plots and true color aerial photographs (1:12,000 and 1: 20,000 scales) to assign each class to one of the five successional stage categories. Fiorella and Ripple (1993) also compared the spectral characteristics of oldgrowth and mature forest and suggested that TM bands 1, 2, and 4; the NDVI; TM 4/3, 4/5, and 4/7 band ratios; and the Tasseled Cap features of brightness, greenness, and wetness for oldgrowth forest were significantly lower than those of mature forest. Cohen *et al.* (1995) estimated and mapped forest age and structure in the Oregon Cascade Range by integrating vegetation structural attribute values with the Tasseled Cap indices and spectral characteristics of several forest classes (young, mature, and old-growth) through regression analysis.

In our study, a spectral pattern matching approach that utilizes the spectral angle concept was used for mapping deforestation and successional stages of forest regrowth in the study area. By calculating spectral angles between finely defined spectral clusters and known reference signatures, and assigning each spectral cluster to one of the reference classes based on the results of spectral angle analysis, we were able to map forest regrowth stages and agricultural land-use classes. Although the cosine of the angle concept is utilized in determining the spectral similarity between image endmembers and image pixels (Center for the Study of Earth from Space, 1993) and the separability between image endmembers (Sohn and McCoy, 1997) for modeling a mixture for unmixing, its concept and applicability for spectral pattern matching are not fully investigated or utilized yet by the remote sensing community. The basic premise of our spectral pattern matching approach is that, even though variations in spectral patterns among the same type of objects caused by different soil color, moisture content, vegetation types and their leaf color, topographic influences, etc., are expected, generally, the same type of objects are assumed to have "similar" pattern (shape) of spectral signatures across the spectral bands.

The Euclidean Distance and the Cosine of the Angle in Feature Space

Multispectral classification is the procedure of grouping image pixels into spectral clusters. Two patterns that represent like objects are expected to be very close to each other in pattern space (Pao, 1989). Based on this simple assumption, pixels are classified in accordance with the class membership of nearest distribution center or cluster center. In conventional multispectral classification, most of the classifiers utilize nearest neighbor rules or Bayesian rules. Nearest neighbor classifiers assign pixels based on the minimum-distance rule. Bayesian classifiers utilize the concept of *likelihood* or *beliefs* that a certain pixel belongs to a certain class membership. Likelihood or beliefs, i.e., *a posteriori* probability, is determined based on *a priori* probability. If we assume that the *a priori* probabilities are equal for all classes, then the decision rule would deduce to the minimum distance. If the *a priori* probabilities are not equal for all classes, the decision rule would take the form of weighted minimum distances (Pao, 1989). Even though several other transformed distance concepts, such as Mahalanobis distance, are developed to overcome limitations of the Euclidean distance, the Euclidean distance is the conceptual foundation of all the conventional classifiers in statistical pattern recognition.

Consider two-dimensional (band x and band y) feature space. Let two spectral signatures, $\mathbf{v}_1$ and $\mathbf{v}_2$, represent differ-

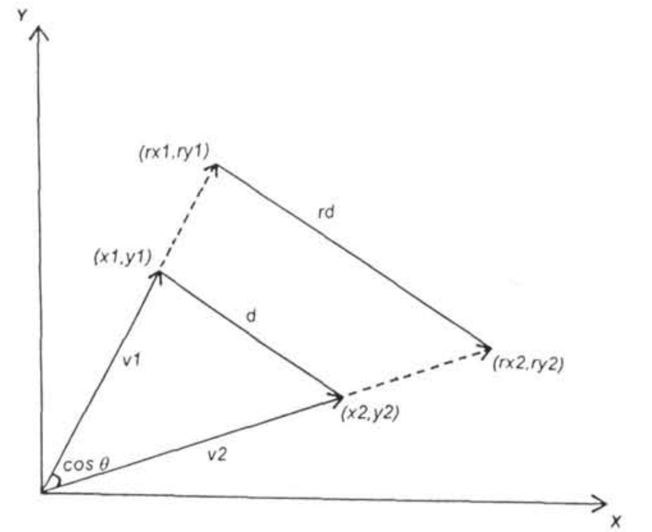

Figure 2. Spectral angle and spectral distance in feature space.

ent surface objects. The two signatures can be plotted in two-dimensional feature space as vectors, $\mathbf{v}_1$ and $\mathbf{v}_2$ (Figure 2). Then the Euclidean distance is the length of the line segment connecting the end points of the two vectors (*d* in Figure 2). The spectral angle is the cosine of the angle between the two vectors (cos θ). If we linearly scale $\mathbf{v}_1$ and $\mathbf{v}_2$ by distance *r*, the spectral distance will be scaled by *r*. On the other hand the cosine of the angle ($\cos\theta$) between the two vectors $\mathbf{v}_1$, $\mathbf{v}_2$ remains same: i.e.,

$$\cos\theta_{v1,\ v2} = \frac{\mathbf{v}_1^T\mathbf{v}_2}{\|\mathbf{v}_1\|\|\mathbf{v}_2\|}.$$

If we scale the length of vectors by *r*, then both numerator and denominator are multiplied by *r*, and the $\cos\theta$ is unchanged (Strang, 1980). The same will be true for feature space spanned by more than two bands. Two spectra will be *exactly* linearly scaled versions of one another when one spectra is vertically shifted downward or upward by DN levels, or distance *r* (Guo and Moore, 1993). In reality, the spectra of the same type of surface object are *approximately* linearly scaled versions of one another due to the atmospheric and topographic variations (Guo and Moore, 1993). So the actual vectors in feature space will fall slightly above or below the linearly scaled vectors. But the changes in the cosine of the angle caused by this variance remain very small. Due to this invariant nature of the cosine of the angle to the linearly scaled variations, it becomes sensitive to the pattern (shape) of the spectral signatures across the spectral bands and gives a better definition of "similarity" of spectral pattern. Discussion on the concept and nature of the cosine of the angle in feature space is found in Sohn and McCoy (1997).

The sensitivity of the spectral distance and the cosine of the angle to the spectral pattern was tested using soil and sagebrush field spectra (Figures 3 and 4) taken in Long Valley, Nevada during August 1993. Field spectra were measured using the SE590 field spectrometer. The 252-band raw data were calibrated to reflectance using the standard panel measurements taken prior to scanning each data set and convolved with a TM bandpass filter (TM bands 1, 2, 3, and 4). Thirty-five soil reflectrance spectra and 28 sagebrush reflectance spectra were used for the test. Mean reflectance spectra of soil and sagebrush were provided as reference spectra. Data collection and calibration methods are presented in Sohn (1994). Euclidean distances, Mahalanobis distances, and the cosine of the angles between the two reference spectra and the provided soil and sagebrush spectra are calculated. Mahalanobis distance was used as an example of the transformed Euclidean distance. Calculated spectral distances and the cosine of the angles are in Tables 1 and 2. Even though soil spectra show variances in reflectance value between dark and light colored soil, as in Figure 3, the variance is approximately linearly scaled. They do not show great interband contrast and they are relatively flat. All soil spectra show similar reflectance patterns across the spectral bands. Contrary to the soil spectra, sagebrush spectra show great interband contrast and have unique reflectance patterns across the spectral bands that can be easily distinguished from soil spectra. All the sagebrush spectra are also approximately linearly scaled versions of one another. Because the two groups of spectra are well defined typical soil and vegetation spectra, it is expected that all the soil spectra would have closer distances to mean soil spectra and all the sagebrush spectra are closer to mean sagebrush spectra.

According to the measured Euclidean distances in Table 1, however, five out of 35 soil spectra show the closer distances to mean sagebrush spectra. Even though the rest of

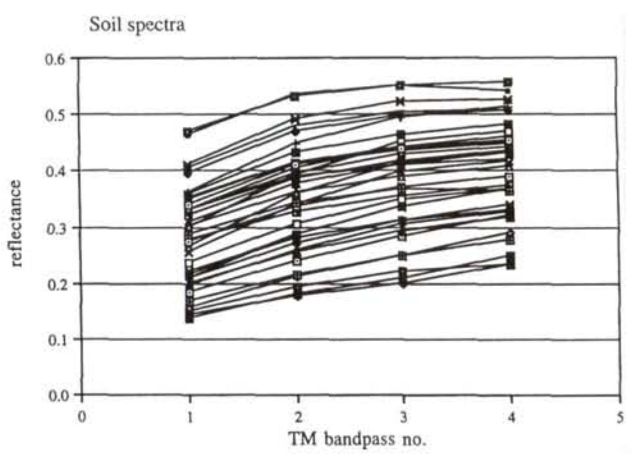

Figure 3. Soil TM Bandpass Spectra.

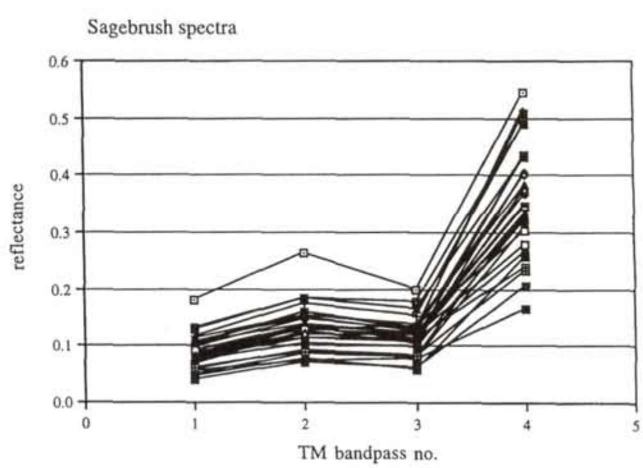

Figure 4. Sagebrush TM Bandpass Spectra.

Table 1. Spectral Distances between Provided Known Spectra and Reference Spectra

Soils	Distance to soil ref. spectrum	Distance to sagebrush ref. spectrum	Sagebrushes	Distance to soil ref. spectrum	Distance to sagebrush ref. spectrum
soil1	19.55 (31.58)	22.24 (105.15)	sagebrush1	40.2 (168.93)	1.46 (0.52)
soil2	14.75 (10.41)	26.84 (135.11)	sagebrush2	41.53 (151.87)	5.10 (6.62)
soil3	30.94 (29.54)	18.47* (82.08)	sagebrush3	52.68 (143.71)	18.03 (12.69)
soil4	25.88 (20.42)	17.68* (91.96)	sagebrush4	37.05 (251.67)	7.87 (6.14)
soil5	31.98 (50.61)	15.79* (56.89)	sagebrush5	50.64 (176.33)	13.68 (8.09)
soil6	10.66 (34.48)	48.42 (318.84)	sagebrush6	42.41 (120.48)	8.29 (8.53)
soil7	17.61 (17.73)	24.33 (109.84)	sagebrush7	40.33 (114.30)	2.53 (21.29)
soil8	4.92 (31.87)	41.97 (334.97)	sagebrush8	46.03 (285.65)	6.67 (16.00)
soil9	10.93 (11.76)	29.58 (188.16)	sagebrush9	37.85 (263.54)	15.35 (15.84)
soil10	11.32 (15.93)	29.32 (195.94)	sagebrush10	39.25 (127.09)	3.44 (8.25)
soil11	25.25 (34.67)	19.46* (78.71)	sagebrush11	44.35 (106.64)	12.03 (16.53)
soil12	3.71 (26.10)	39.24 (266.09)	sagebrush12	47.38 (262.09)	8.74 (14.30)
soil13	13.23 (1.62)	27.92 (155.64)	sagebrush13	43.05 (213.68)	9.29 (7.00)
soil14	4.51 (11.39)	36.11 (111.79)	sagebrush14	40.61 (200.71)	7.74 (4.66)
soil15	16.51 (21.60)	25.30 (131.66)	sagebrush15	38.40 (224.17)	1.95 (2.96)
soil16	11.14 (2.65)	49.85 (225.13)	sagebrush16	38.09 (331.65)	16.14 (29.87)
soil17	2.30 (1.19)	37.59 (157.54)	sagebrush17	26.84 (200.53)	26.10 (292.39)**
soil18	33.39 (58.75)	16.64* (49.33)*	sagebrush18	39.45 (298.17)	1.13 (20.88)
soil19	8.99 (1.58)	48.10 (211.13)	sagebrush19	31.59 (322.99)	15.84 (46.06)
soil20	7.09 (12.74)	46.36 (223.30)	sagebrush20	37.20 (178.70)	4.78 (0.94)
soil21	16.02 (4.80)	54.51 (234.62)	sagebrush21	52.64 (159.29)	20.92 (16.37)
soil22	7.94 (4.18)	32.50 (178.01)	sagebrush22	39.53 (159.09)	5.91 (6.21)
soil23	5.68 (0.47)	44.76 (199.90)	sagebrush23	35.62 (193.38)	4.59 (0.20)
soil24	2.51 (2.09)	41.83 (165.77)	sagebrush24	40.87 (250.99)	2.24 (5.95)
soil25	12.18 (8.52)	51.17 (238.96)	sagebrush25	43.59 (301.91)	5.21 (24.51)
soil26	20.24 (23.25)	58.35 (323.57)	sagebrush26	34.37 (254.66)	14.41 (13.45)
soil27	4.24 (15.23)	38.07 (227.86)	sagebrush27	48.41 (187.06)	13.97 (6.23)
soil28	11.64 (14.09)	50.59 (232.31)	sagebrush28	31.48 (139.01)	10.98 (7.14)
soil29	26.72 (38.02)	65.09 (361.27)			
soil30	7.17 (2.84)	46.20 (212.67)			
soil31	33.98 (74.06)	72.47 (404.50)			
soil32	23.85 (47.95)	62.43 (364.12)			
soil33	11.25 (9.08)	50.11 (240.22)			
soil34	22.76 (20.72)	61.29 (299.42)			
soil35	34.87 (19.98)	73.04 (239.66)			

1. Distances are multiplied by 100 for easy comparison.
2. Numbers inside the parenthesis are Mahalanobis distances. Mahalanobis distances were calculated using the equation $D_{ij} = \sqrt{[(X_i - \mu_j)^T \xi^{-1} (x_i - \mu_j)]}$, where ξ is the common covariance matrix and μ_j is the group mean.
*Soil spectra that have closer distance to sagebrush mean spectra.
**Sagebrush spectrum that has closer distance to mean soil spectra.

the soil spectra, 30 out of 35 spectra, show relatively closer distances to mean soil spectra, the Euclidean distance values do not show any systematic or consistent relations to the similarity of the spectral pattern. According to the calculated Mahalanobis distances in Table 1, one soil spectrum is closer to the mean sagebrush spectra and one sagebrush spectrum shows a closer distance to the mean soil spectra. Although Mahalanobis distance improved classification accuracy greatly by considering variance of the data distribution, it is extremely sensitive to data normality. This is why we often get unreliable classification results when a parametric rule is used with image data that are away from a normal distribution. On the other hand, Table 2 shows that, when the cosine of the angles are used for pattern mapping, all the soil spectra show closer angles to the mean soil spectra and all the sagebrush spectra show closer angles to the mean sagebrush spectra. The cosine of the angles between the provided known spectra and the reference spectra show very consistent relation to the similarity of spectral pattern (shape). The angles are consistently narrow among the spectra that have similar patterns. When patterns are not similar, the angles become consistently wider.

Image Data

Due to the seasonal variations of spectral signatures, in change detection using remotely sensed digital image data, the date of data acquisition is important. In this study, Landsat 5 TM images from 27 April 1985 and 03 December 1995 were used for analysis. Both images were acquired during one of the dry seasons. Both April and December fall into the same agricultural cycle, after harvest and before planting of corn. Due to the severe drought in Spring of 1995, trees in most of the study area were defoliated, and that made the distinction between forest and agricultural area difficult. Accordingly, the December 1995 image was chosen for the analysis instead of available March 1995 image data. The severe spring drought was followed by Hurricane Roxanne during 10–17 October 1995. We compared the image scene before the hurricane (March 1995) with the image scene after the hurricane (December 1995) and we did not see any evidence of structural damage of forest in the study area in the December 1995 image. This was also confirmed in the field through interviews with *ejidatarios*. Tree recovery from the severe drought was rapid because the hurricane provided precipitation and caused no structural damage of trees. For our study, images of two different dates were not calibrated to reflectance. They were analyzed independently, and no spectral comparison between the two dates was attempted. In both the 1985 and the 1995 images, several, small patches of cloud cover and cloud shadow were present. Because there is no significant seasonal variation in temperature in the study area, precipitation and the agricultural cycle are the

TABLE 2. THE COSINE OF THE ANGLES (COS θ) IN DEGREES BETWEEN PROVIDED KNOWN SPECTRA AND REFERENCE SPECTRA

Soils	Angles to soil ref. spectrum	Angles to sagebrush ref. spectrum	Sagebrushes	Angles to soil ref. spectrum	Angles to sagebrush ref. spectrum
soil1	4.32	23.84	sagebrush1	26.57	0.88
soil2	2.13	26.00	sagebrush2	32.48	5.41
soil3	1.86	26.26	sagebrush3	29.99	3.05
soil4	5.31	22.53	sagebrush4	28.83	1.96
soil5	5.23	22.53	sagebrush5	33.84	6.64
soil6	2.17	26.33	sagebrush6	22.32	5.13
soil7	2.56	25.30	sagebrush7	26.02	1.49
soil8	2.77	25.99	sagebrush8	33.90	6.74
soil9	3.67	24.81	sagebrush9	31.77	4.55
soil10	4.02	24.72	sagebrush10	23.72	3.52
soil11	3.02	24.87	sagebrush11	19.64	7.71
soil12	2.95	25.93	sagebrush12	33.86	6.88
soil13	1.52	26.00	sagebrush13	21.93	5.53
soil14	1.06	27.62	sagebrush14	32.78	5.62
soil15	3.10	25.46	sagebrush15	24.82	2.72
soil16	0.39	27.49	sagebrush16	32.11	4.90
soil17	0.18	27.18	sagebrush17	22.11	6.25
soil18	3.38	23.98	sagebrush18	27.75	1.01
soil19	1.10	28.09	sagebrush19	25.45	2.00
soil20	2.24	28.87	sagebrush20	27.35	0.28
soil21	1.09	27.81	sagebrush21	19.86	7.48
soil22	1.77	26.33	sagebrush22	21.41	6.02
soil23	0.30	27.34	sagebrush23	24.44	2.91
soil24	1.08	27.81	sagebrush24	30.04	2.85
soil25	1.75	28.52	sagebrush25	29.15	2.24
soil26	0.30	27.43	sagebrush26	28.04	0.84
soil27	2.29	29.24	sagebrush27	25.64	1.71
soil28	2.16	28.59	sagebrush28	23.25	4.04
soil29	2.00	28.83			
soil30	0.80	27.61			
soil31	4.00	30.37			
soil32	2.59	29.22			
soil33	1.35	28.01			
soil34	2.12	28.85			
soil35	3.66	29.67			

major factors that contribute to changes in spectral signatures.

Field Data

Field data were collected during May and early June of 1996. Sample sites for identifying forest regrowth stages and for accuracy assessment were located through the interviews with the certified *ejidatarios* of 122 households (207 *ejido* plots) in seven *ejidos*. Sample households were selected by stratified random sampling by *ejido* and their lots were located in the field. Forest regrowth stages were identified by the age of fallow (Table 3). Identified forest regrowth stages include initial secondary succession (SS1), intermediate secondary succession (SS2), and advanced secondary succession (SS3). We assumed that the structural characteristics of different regrowth stages of forest under a given environment will be determined by the age of fallow. SS1 corresponds to *Sak'aab'kool*. SS2 corresponds to *Kambal-hubché*. Both *Kanalhubché* and *Kelenché* are combined in SS3. Because most of the forests in the study area were younger than 16 years, we determined that it was not practical to identify *Kelenché* as a separate successional stage.

The 1995 image was georeferenced using five quadrangles of 1:50,000-scale topographic maps that cover most of the study area. Out of 33 ground control points, 11 were used for registering the 1985 and 1995 images to UTM coordinates with 1.48 and 0.97 RMS errors, respectively. The color composites of the georeferenced TM image scenes of the study area were printed approximately at 1:33,000 scale with UTM coordinates. Sample sites were located and identified in the field with the help of a Magellan Fieldpro V GPS and local farmers. We used hardcopy image scenes of our study area for field survey because the 1:50,000-scale topographic maps are the largest scale maps of the study area and they do not provide recent information in detail. Cleared *milpas*, recently abandoned agricultural field/stubble, SS1, SS2, SS3, several old forest patches (40 and 100 years), ranches, urban areas, and any developed facilities such as a large hogfattening facility that is bigger than TM spatial resolution were identified and located in the field, and the age of the fallow and estimated height of stands were recorded for each site. Recently abandoned agricultural field/stubble includes harvested first- and second-year *milpas* that are not cleared or burnt. First-year *milpas* will be cultivated one more year after clearing and burning. Harvested second-year *milpas* will be abandoned and forest regrowth will start. These first- and second-year *milpas* were not spectrally separable. In either case, because both are recently cultivated fields, they are regarded as agricultural fields. Data collected from 43 sites were used as references and the rest were reserved for accuracy assessment.

TABLE 3. FOREST REGROWTH STAGES AND THE AGE OF FALLOW

Forest Regrowth Stages	Age of Fallow	Canopy Height
Initial Secondary Succession (SS1)	2–5 years	1–3 m
Intermediate Secondary Succession (SS2)	6–10 years	5–8 m
Advanced Secondary Succession (SS3)	11–30 years	10–15 m

Mapping Approach

Utilizing the conceptual difference between the spectral distance and the spectral angle in feature space, we first generated very narrowly defined spectral clusters of the study area image data using the ISODATA classifier. Then the spectral angles between the narrowly defined spectral clusters and known reference signatures were calculated for spectral pattern matching. All seven TM bands were used for classifications of the images and calculating spectral angles. The procedures involved in mapping land cover using the spectral angle concept in this study include

- First, narrowly defined spectral clusters (200 spectral clusters) were generated using the ISODATA classification rule for the 1985 and the 1995 study area images;
- Reference signatures were collected from the known sites;
- Spectral patterns of collected reference signatures were examined and separability between the reference signatures was tested;
- The cosine of the angles between the 200 spectral clusters and the collected reference signatures were calculated; and
- Each spectral cluster was assigned to one of the information classes based on the spectral angle analysis between the spectral clusters and the provided reference signatures.

To collect the reference signatures, first all 43 reference sample sites identified in the field were located on the 1995 study area image, and reference signatures of different land-cover types were collected. The reference signatures collected include urban center, paved highways, major roads, urban roads, bright rooftops, waterbody, cloud, cloud shadow, cleared agricultural field, abandoned field/stubble, SS1, SS2, SS3, and mature forest. Cloud and cloud shadow were identified directly from the image, and signatures were collected. For SS1, reference signatures were collected from the sites which have fallow ages of 2 to 3 years. Reference signatures of SS2 were collected from the sites which have fallow ages of 6 to 10 years. Reference signatures of SS3 were collected from the sites which have fallow ages of 15 to 20 years. For mature forest, reference signatures were collected from the identified 40-year and 100-year patches. For each land-cover type, one to seven reference signatures were collected depending on the spectral variability of the feature across the study area scene. Instead of averaging the collected reference signatures to acquire a representative reference signature for each land cover/use type, we provided one to seven signatures for each land cover/use type to cover the variance caused by topographic and environmental factors. The spectral pattern of all the reference signatures were examined and separabilities between the reference signatures were tested using transformed divergence distance. Generally, transformed divergences less than 1500 are considered indiscriminable (Steininger, 1996). For 1995 reference signatures, transformed divergence distances between the reference signatures of mature forest and SS3 show extremely low values that range from 586 to 948 and were considered not distinctive from one another. Accordingly, the mature forest and SS3 are merged into the same land-cover class as advanced secondary succession/mature forest at the final merging stage. It appears that this is because of the similar tree stand structure of mature forest and advanced secondary succession. For 1995, a total of 37 reference signatures for 12 different land cover/use features were collected and provided for spectral angle measurement. These include SS1 (3), SS2 (5), SS3 (4), cloud (2), cloud shadow (1), cleared agricultural fields (7), abandoned/stubble (2), water (1), paved highway (1), major road (1), urban road (3), urban center (1), rooftop (1), and mature forest (5). Inside the parentheses are the numbers of reference signatures collected for each land-cover type.

For 1985, because there were no available aerial photographs or other ancillary data to help in collecting reference signatures, some reference sites were identified and reference signatures were collected using land-use and management history. For advanced secondary succession/forest land-cover classes, reference signatures were collected from the sites that were identified as old forest patches (40 years and 100 years) in private ranches and the forest reserve that surround the town of Yaxcaba. The forest reserve is known to have been preserved at least for 30 years at the time of field survey in the summer of 1995. For collecting reference signatures of SS1 and SS2, we first located all the available reference sites with the ages of fallow. Then the ages of fallow were subtracted by ten. For example, a 20-year-old forest patch in 1995 is considered as a 10-year-old forest patch in 1985 and, accordingly, identified as SS2. A 15-year-old forest patch should be at the SS1 stage ten years earlier. For urban/developed, cleared agricultural fields, abandoned/stubble, waterbody, cloud, and cloud shadow, we were able to identify directly from the 1985 study area image scene through visual analysis and examining spectral patterns. For 1985, a total of 29 reference signatures for 12 different land cover/use types were provided for spectral angle analysis. These include SS1 (4), SS2 (3), advanced secondary succession/forest (4), cleared agricultural field (5), abandoned/stubble (1), cloud (4), cloud shadow (1), water (1), major road (1), urban (3), urban center (1), and urban road (1). According to the transformed divergence distances, all of the 1985 reference signatures appeared to be separable between different types of land cover. Tables 4a and 4b are the reference signatures representing successional stages of forest regrowth for 1985 and 1995.

TABLE 4A. SPECTRAL RESPONSES (DN VALUES) OF FOREST REGROWTH STAGES IN SOTUTA, YUCATAN, 1985

Forest regrowth stages	TM Bands						
	1	2	3	4	5	6	7
SS1.1	96.32	42.00	40.06	121.41	119.12	153.67	40.51
SS1.2	92.04	39.64	35.20	121.72	116.32	153.28	37.60
SS1.2	90.38	39.82	34.20	126.64	108.92	152.12	34.28
SS1.4	93.29	41.03	37.18	120.18	120.18	152.88	41.22
SS2.1	87.44	37.05	29.33	134.44	83.22	148.00	22.38
SS2.2	85.86	37.06	29.05	137.02	80.62	147.94	21.26
SS2.3	87.04	37.95	29.89	136.91	85.70	149.42	22.72
SS3.1	83.98	32.99	27.09	120.77	78.95	147.84	21.31
SS3.2	84.01	32.99	27.01	119.04	78.06	149.55	21.44
SS3.3	87.20	37.31	29.75	126.24	80.25	146.61	21.96
SS3.4	85.12	35.89	27.87	126.40	76.02	146.87	20.21

SS1: initial secondary succession, SS2: intermediate secondary succession, SS3: advanced secondary succession. Following the decimal represents the number of signatures for each successional stage.

TABLE 4B. SPECTRAL RESPONSES (DN VALUES) OF FOREST REGROWTH STAGES IN SOTUTA, YUCATAN, 1995

Forest regrowth stages	TM Bands						
	1	2	3	4	5	6	7
SS1.1	45.85	16.42	14.14	56.07	44.35	135.92	11.21
SS1.2	45.45	16.75	13.56	61.32	44.81	134.16	10.81
SS1.3	47.30	17.61	14.07	60.46	44.23	134.23	10.61
SS2.1	45.17	16.78	13.48	60.39	42.00	135.31	10.02
SS2.2	44.55	16.36	12.36	62.48	41.00	132.58	9.31
SS2.3	44.40	15.93	12.37	60.34	40.65	132.18	9.21
SS2.4	44.84	16.49	13.21	59.96	42.07	134.25	9.80
SS2.5	45.73	17.06	13.40	62.62	41.21	133.54	9.47
SS3.1	44.50	15.92	12.35	53.78	37.85	134.14	8.85
SS3.2	44.12	16.07	12.36	51.73	37.61	134.25	9.34
SS3.3	43.92	15.73	11.69	53.38	39.80	133.61	9.50
SS3.4	43.96	15.70	11.78	53.32	39.47	133.37	9.29

According to the collected reference signatures, SS1 shows higher spectral response in visible bands with low green/red (TM bands 2/3) ratio, and very high spectral response in moisture absorption bands (TM bands 5 and 7). With its young trees, SS2 shows higher spectral response in the near infrared band (TM band 4) with higher green/red and IR/red ratios, which is consistent with increased biomass. The spectral response in moisture absorption bands is decreased compared to SS1 due to increased plant moisture. With developed multicanopy structure and higher biomass, SS3 shows the lowest spectral responses in the green, red, and near infrared bands compared to SS1 and SS2 due to the shade effect resulting from a developed multicanopy structure. In the moisture absorption bands, SS3 also shows that the lowest spectral response due to increased plant and soil moisture content resulted from the increased biomass and developed multicanopy structure that prevent the evaporation of soil moisture. We can see that the spectral response characteristics of forest regrowth stages in the study area, the maize region in Yucatan, are similar to the patterns observed by Mausel *et al.* (1993) in the Amazon in spite of the differences in climate, soil conditions, and vegetation between the two areas.

Once reference signatures were collected, 200 spectral clusters were generated using the ISODATA classification rule for both the 1985 and 1995 images of the study area. Then, spectral angles between the 200 spectral clusters and the provided reference signatures were calculated. Each of the 200 spectral clusters was assigned to one of the reference classes based on the minimum spectral angle rule. Once each cluster is assigned to one of the reference classes, spectral clusters that belong to the same land cover/use type are merged together into nine categories of land cover/use types: urban/developed, cleared agricultural field, abandoned/stubble, initial secondary succession, intermediate secondary succession, advanced secondary succession/mature forest, waterbody, cloud, and cloud shadow.

Deforestation and Agricultural Land-Use Changes in the Study Area

The classified land cover/use maps of 1985 and 1995 are shown in Plates 1a and 1b. Land-cover/land-use change is summarized in Table 5. The calculated mapping accuracies are shown in Tables 6a (1985) and 6b (1995). For accuracy

TABLE 5. LAND-USE/LAND-COVER CHANGE IN NORTH-CENTRAL YUCATAN (1985–1995)

	1985		1995	
	Hectares	(%)	Hectares	(%)
Urban/Developed	374.31		557.19	
Agriculture	21,921.30	(17.52)	39,015.91	(31.23)
ClearedField	11,997.45	(9.59)	15,612.57	(12.13)
Abandoned/Stubble	9,923.85	(7.93)	23,888.34	(19.10)
Initial Secondary Succession	44,011.26	(35.17)	31,660.20	(25.32)
Intermediate Secondary Succession	6,801.84	(5.43)	17,555.40	(14.04)
Advanced Secondary Succession/Forest	51,562.26	(41.21)	35,691.57	(28.54)
Water	—		15.75	
Cloud	292.41		336.87	
Cloud Shadow	150.84		177.03	
Total*	125,114.22	(100.00)	125,044.92	(100.00)

*Total area is the image subset area shown in Plates 1a and 1b.

TABLE 6A. ERROR MATRIX FOR LAND-USE/LAND-COVER MAP OF SOTUTA, YUCATAN 1985

		Interpreted Land Use (classified)												
		1	2	3	4	5	6	7	8	9	Total	Omission Error (%)	Commission Error (%)	User's Accuracy (%)
	1	9				2					11	18.19	35.72	81.81
	2										—	—	—	—
Actual	3	1		10							11	9.09	0.00	90.91
Land	4				9						9	0.00	0.00	100.00
Use	5	4				24					28	14.29	7.70	85.71
	6						21				21	0.00	0.00	100.00
	7							23			23	0.00	4.17	100.00
	8							1	17		18	5.56	0.00	94.44
	9									28	28	0.00	0.00	100.00
Total		14	—	10	9	26	21	24	17	28	149			94.63

TABLE 6B. ERROR MATRIX FOR LAND-USE/LAND-COVER MAP OF SOTUTA, YUCATAN 1995

		Interpreted Land Use (classified)												
		1	2	3	4	5	6	7	8	9	Total	Omission Error (%)	Commission Error (%)	User's Accuracy (%)
	1	11		3		1					15	26.67	15.39	73.33
	2		10		1						11	9.10	0.00	90.90
Actual	3			5							5	0.00	50.00	100.00
Land	4				8						8	0.00	11.12	100.00
Use	5	2		2		17					21	19.05	10.53	80.95
	6					1	36				37	2.71	5.27	97.29
	7						2	39			41	4.88	4.88	95.12
	8							2	30		32	6.25	0.00	93.75
	9									30	30	0.00	0.00	100.00
Total		13	10	10	9	19	38	41	30	30	200			93.00

1. Urban/Developed, 2. Water, 3. Cloud, 4. Cloud Shadow, 5. Cleared Field, 6. Abandoned/Stubble, 7. Initial Secondary Succession, 8. Intermediate Secondary Succession, 9. Advanced Secondary Succession/Forest.

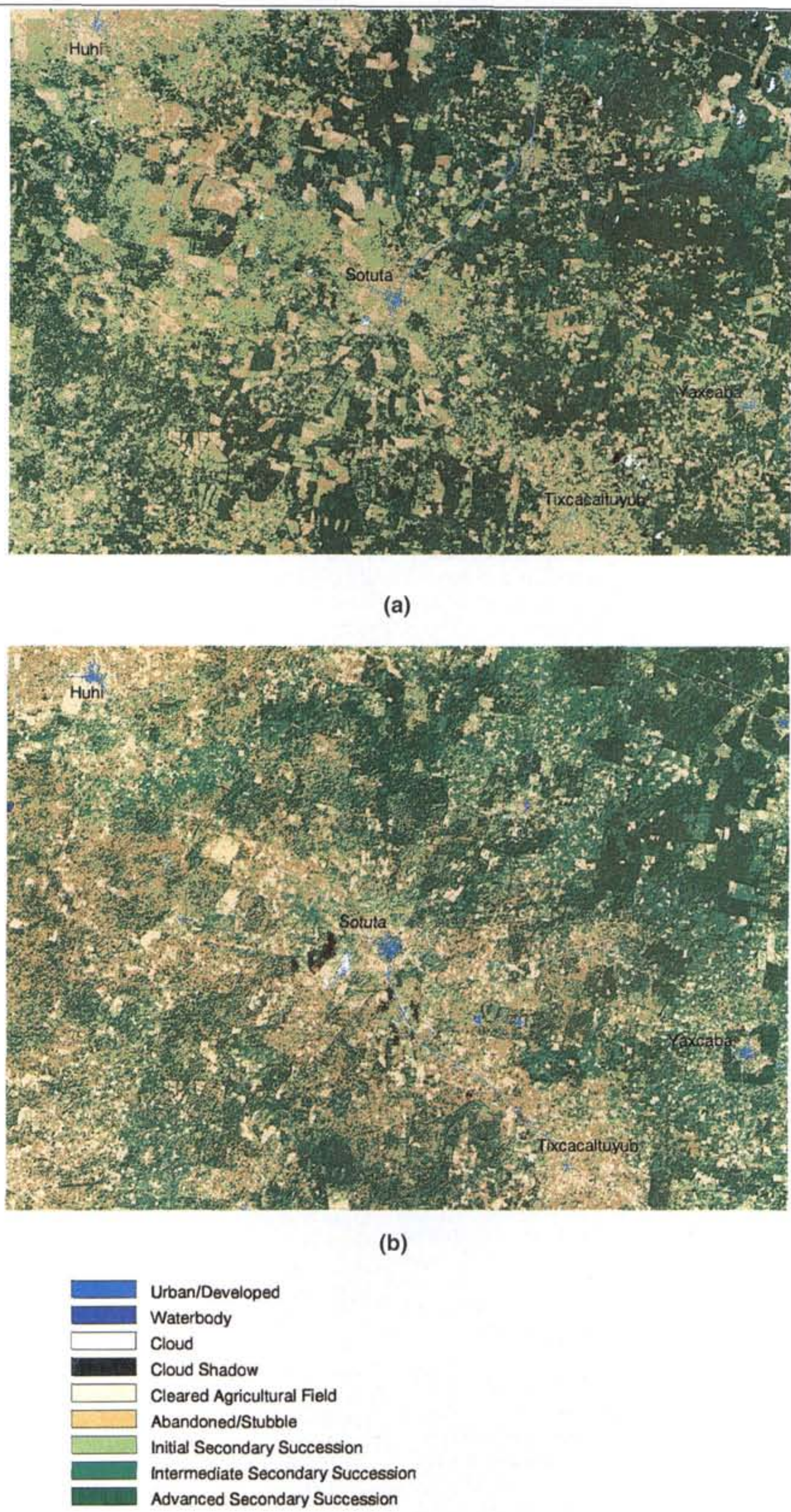

Plate 1. (a) Forest regrowth stages and agricultural land use in Sotuta, Yucatan, 1985. (b) Forest regrowth stages and agricultural land use in Sotuta, Yucatan, 1995.

assessment, 350 stratified (by land cover/use class) random sample points were generated. Then, the generated random sample points were compared with ground data, and the sample points only fell within the lots or patches for which ground data exist were kept. This was inevitable due to the limited ground truth and ancillary data for 1985 and the difficulty of going back to field for additional survey. For 1985, cloud, cloud shadow, urban/developed, cleared agricultural fields, abandoned/stubble classes were identified on color infrared composite images of study area. For identifying secondary regrowth stages, the same methods used for collecting reference signatures were used. The resulting sample points were 149 for 1985 and 200 for 1995. The overall accuracy was 94.6 percent for 1985 and 93.0 percent for 1995. For 1985, advanced secondary succession/forest, cloud shadow, abandoned/stubble, initial secondary succession classes show 100 percent accuracy. For 1995, cloud, cloud shadow, and advanced secondary succession/forest classes show 100 percent accuracy. For cloud and cloud shadow, when stratified random sampling points were generated, because there were only a couple of small patches of cloud and cloud shadow present in the study area images, all the sample points were generated within the areas that were classified as cloud and cloud shadows. Accordingly, cloud and cloud shadow show 100 percent accuracies on both 1985 and 1995 error matrices. Kappa values for 1985 and 1995 error matrices are 0.93 and 0.91, respectively. In general, forest regrowth stages and agricultural fields are mapped with higher accuracies, and urban/developed classes show lower accuracies. Some areas covered with thin clouds were confused mostly with urban/developed and cleared agricultural fields. Some urban/developed areas were confused mostly with cleared agricultural fields.

According to the mapping results, in 1985, approximately 44,011 hectares, or 35 percent of the study area, were in initial secondary succession. In contrast, only 6,801 hectares, or 5 percent of the study area, were in intermediate secondary succession. This indicates that, even though deforestation in the study area started in the early 1900s, extensive forest clearings started in the late 70s and early 80s. In 1985, about 21,921 hectares, or 17 percent of the study area were cultivated for agriculture. About 41 percent of the study area, or 51,562 hectares, were still covered by advanced secondary succession or forest. In 1995, roughly 39,015 hectares were in initial secondary succession, decreasing to 25 percent from 35 percent in 1985. Intermediate secondary succession increased to 17,555 hectares, or 14 percent of the study area, from 6,801 hectares, or 5 percent in 1985. This indicates that some of the initial secondary succession in 1985 developed into intermediate secondary succession. Advanced secondary succession/forest has decreased to 35,691 hectares, or 28 percent of total area, from 51,562 hectares, or 41 percent in 1985. In 1995, about 39,015 hectares, or 31 percent of total area, were cultivated for agriculture, nearly twice the area in agricultural land use than in 1985.

The results of this study suggest that extensive and massive forest clearings occurred in the late 1970s and continues in the study area, and that agricultural land use has intensified in the last ten years. The 1995 land-cover/land-use map (Plate 1b) shows that most of the advanced secondary succession and forests are found within either communal forest reserves or in private ranches. Outside of these forest reserves and private ranches forest fragmentation appears severe. Especially along the corridors of major urban areas (Sotuta, Huhi, and Tixcacaltuyub), all the lands are intensively cultivated for agriculture. Forests are mainly small, fragmented patches of various stages of secondary regrowth. No patches of mature forest of any significant size remain. These results of land-cover/land-use change analysis are consistent with suggestions and implications of other related studies (Gomez-Pompa, 1987; Chemas and Rico-Gray, 1991; Gates 1993; Re Cruz, 1996). Miranda (1958; cited in Rico-Gray *et al.* (1988)) reported that the vegetation in the study area was a medium-height (canopy height 25m) tropical deciduous forest, *selva mediana decidua.* Studies by Roldan (1985; reported in Rico-Gray *et al.* (1988)) report the vegetation in the same region as low-height (canopy height 10 to 12m) tropical deciduous forest, *selva baja caducifolia.* Rico-Gray *et al.* (1988) suggested that the age of the most vegetation patches in the area (Tixcacaltuyub) varies between one and 40 years. In 1991, Chemas and Rico-Gray report that the age of the vegetation in the same area varies between one and 20 years. According to our observation, canopy heights for relatively old forest patches (40 years and 100 years) reached 20 meters. Canopy heights for most of the forests in advanced successional stage were about 10 meters.

The decline of forest in the study area is of concern to *milperos* as well as to other concerned parties because it implies the loss of important resources. Mexican government development agencies tend to regard traditional shifting agriculture as the most ecologically destructive activity (Gates, 1993). Gates (1993) and Gomez-Pompa (1987) argue that shifting agriculture is not inherently destructive of forest land in itself. They regard the agricultural development projects initiated by the government development agencies that encourage modern agricultural inputs, development of pastures for cattle, and commercial logging operations without considering environmental constraints and sustainability as the major causes of extensive destruction of forest in the study area. According to Gates (1993), the Maya *milpa* system is a highly efficient and sustainable agricultural system, given the environmental constraints, as long as sufficient land per person can be held in reserve to maintain a viable fallow period. Gomez-Pompa (1987) suggests that the Maya were able to support population densities of 100 to 200 people per square kilometer in *milpa* agriculture and up to 700 to 1,150 for the more intensively cultivated areas while preserving biological diversity and without extensive forest clearings.

Conclusions

Using a new spectral pattern matching approach with the two dates of Landsat TM data, we were able to map deforestation, secondary regrowth stages of forest, and changes in the intensity of agricultural land use with high accuracy in the maize region of the state of Yucatan. According to our study results, in the study area, the rate of deforestation is high and agricultural land use is intensifying increasingly. Population growth, limited amount of land available for slash and burn shifting agriculture, and agricultural development policies that encourage commercialization of agriculture and cattle grazing seem to be major causes of deforestation in the study area. Further studies are needed for increased understanding of the impacts of agricultural development policy on deforestation in the study area. We believe that our study results will provide baseline data for understanding the impacts of Article 27 in the near future in the study area.

According to our analysis, it seems that TM data carry more information than most of the studies suggest, and that the spatial and spectral resolution of TM data is fine enough for addressing most of the environmental and ecological problems and for mapping natural resources. To compare the classification results of the maximum likelihood classifier (MLC) and the spectral pattern matching approach used in this study, we provided the reference signatures that were used for spectral pattern matching as the training signatures for the MLC and performed classifications. The results were less than satisfactory. The MLC classified a large portion of the cleared agricultural fields as urban/developed. Abandoned/stubble was confused with initial secondary succession. A large portion of abandoned/stubble was classified as cleared agricultural field. Some intermediate secondary succession was confused with initial secondary succession. Even though the method we demonstrated in this paper is conceptually and methodologically simple, our test and mapping results suggest that the concept of the cosine of the angle works well for spectral pattern matching due to its sensitivity to the spectral pattern (shape). When a large number of spectral clusters (more than 100 spectral clusters) were generated, most of the features of interest will be separated. However, it would be extremely difficult to compare, discriminate, and identify the subtle differences in spectral patterns between a large number of spectral clusters through visual examination and assigning them into information classes. According to Ryerson (1989), one of the major problems in conventional digital image classification approaches is the lack of knowledge required of the interpreter for adequate interpretation, which results in a lack of consistency in the result of interpretations. By adapting the spectral pattern matching approach based on the concept of the cosine of the angle, spectral clusters can be assigned into information classes precisely and objectively, and the inconsistency involved in visual identification of a large number of spectral clusters can be avoided. Also, understanding of the nature of feature space, mapping approaches and algorithms, spectral pattern changes caused by environmental and ecological factors, and knowledge in substantive fields seems very important for improving mapping accuracy and for generating useful land cover/use maps.

In this study, the land cover/use change analysis was done without radiometric and atmospheric calibrations of two different dates of image data by collecting reference signatures from both dates of images. However, when images of different dates are calibrated to reflectance through atmospheric correction and radiometric calibration, the method that combines the high dimensional clustering (generating 200 spectral clusters using ISODATA rule) and reference signatures to guide spectral pattern matching may provide a practical way to overcome the lack of data for temporal analysis common for land cover mapping using images of different dates.

Acknowledgments

The authors wish to thank the people of Sotuta for their help in field surveys, as well as collaborators at CINVESTAV — Unidad Merida, especially for Gilberto Balam Pereira, Ernesto Ochoa Estrada, and also for Genny Sonda Ortiz. None of this work would have been possible without the financial support of the National Science Foundation, through grant SBR #9420727. The field survey and the measurement of field spectra used for testing sensitivity to the pattern of spectral signatures were funded through Roger McCoy's Faculty Research Grant and Youngsinn Sohn's Graduate Research Fellowship from the University of Utah. Kenneth Parker helped us through insightful discussions on the concept of the cosine of the angle. None of these agencies or collaborators should be held responsible for the views expressed in this paper. The responsibility lies solely with the authors.

References

Brondizio, E., E. Moran, P. Mausel, and Y. Wu, 1996. Land Cover in the Amazon Estuary: Linking of the Thematic Mapper with Botanical and Historical Data, *Photogrammetric Engineering & Remote Sensing*, 62(8):921–929.

Baños Ramírez, O., 1992. *Campesinos y sociedad ayer y hoy*, Ediciones de la Universidad Autónoma de Yucatán, Mérida, Yucatan, Mexico.

Center for the Study of Earth from Space (CSES), 1993. *SIPS User's Guide: Spectral Image Processing System, Version 1.2*, University of Colorado, Boulder.

Chemas, A., and V. Rico-Gray, 1991. Apiculture and Management of Associated Vegetation by the Maya of Tixcacaltuyub, Yucatan, Mexico, *Agroforestry Systems*, 13:13–25.

Cohen, W.B., T.A. Spies, and M. Fiorella, 1995. Estimating the Age and Structure of Forests in a Multi-Ownership Landscape of Western Oregon, U.S.A., *International Journal of Remote Sensing*, 16(4):721–746.

Duch, G.J., 1992. Condicionamiento ambiental y modernización de la milpa en el estado de Yucatán, *La modernización de la milpa: Utopía o realidad* (D.V. Zizumbo, C.H. Rasmussen, L. Arias, and S. Terán, editors), CICY, Mérida, Yucatan, Mexico, pp. 81–96.

Fiorella, M., and W.J. Ripple, 1993. Determining Successional Stage of Temperate Coniferous Forests with Landsat Satellite Data, *Photogrammetric Engineering & Remote Sensing*, 59(2):239–246.

Gates, M., 1993. *In Default: Peasants, the Debt Crisis, and the Agricultural Challenge in Mexico*, Westview Press, Boulder.

Gomez-Pompa, A., 1987. On Maya Silviculture, *Mexican Studies*, 3: 1–17.

Guo, J.G., and J. McM. Moore, 1993. Cloud-Shadow Suppression Technique for Enhancement of Airborne Thematic Mapper Imagery, *Photogrammetric Engineering & Remote Sensing*, 59(8): 1287–1291.

Ku, R.N., 1992. La milpa yucateca y sus inovaciones tecnológicas, *La modernización de la milpa: Utopía o realidad* (D.V. Zizumbo, C.H. Rasmussen, L. Arias, and S. Terán, editors), CICY, Mérida, Yucatan, Mexico, pp. 267–277.

Mausel, P., Y. Wu, Y. Li, E.F. Moran, and E.S. Brondizio, 1993. Spectral Identification of Successional Stages Following Deforestation in the Amazon, *Geocarto International*, (4):61–71.

Miranda, F., 1958. Estudios de la vegetacion, *Los Recuros Naturales del Sureste y su Aprovechamiento, Vol. 2* (E. Beltran, editor), IMRNR, Mexico, D.F., pp. 213–272.

Moran, E.F., E. Brondizio, P. Mausel, and Y. Wu, 1994. Integrating Amazonian Vegetation, Land-use, and Satellite Data, *BioScience*, 44(5):329–338.

Munguía, M.E., 1994. The Stepchildren of Conasupo: An Independent Regional Marketing System in Central Veracruz, *Economic Restructuring and Rural Subsistence in Mexico: Corn and the Crisis of the 1980s* (C.H. de Alcántara, editor), The Center for US-Mexican Studies, University of California, San Diego, pp. 62–80.

Pao, Y-H., 1989. *Adaptive Pattern Recognition and Neural Networks*, Addison-Wesley, Reading, Massachusetts.

Re Cruz, A., 1996. *The Two Milpas of Chankom: A Study of Socioeconomic and Political Transformations in a Maya Community*, State University of New York Press, Albany.

Rico-Gray, V., and J.G. Garcia-Franco, 1991. The Maya and the Vegetation of the Yucatan Peninsula, *Journal of Ethnobiology*, 11(1): 135–142.

Rico-Gray, V., J.G. Garcia-Franco, A. Puch, and P. Sima, 1988. Composition and Structure of a Tropical Dry Forest in Yucatan, Mexico, *International Journal of Ecology and Environmental Science*, 14:21–29.

Roldan, L.A., 1985. *Flora melifera de la zona de Tixcacaltuyub, Yucatan*, Tesis de Licenciatura, Faculted de Ciencias, UNAM, Mexico, D.F.

Ryerson, R., 1989. Image Interpretation Concerns for the 1990s and Lessons from the Past, *Photogrammetric Engineering & Remote Sensing*, 55(10):1427–1430.

Sader, S.A., R.B. Waide, W.T. Lawrence, and A.T. Joyce, 1989. Tropical Forest Biomass and Successional Age Class Relationships to a Vegetation Index Derived from Landsat TM Data, *Remote Sensing of Environment*, 28:143–156.

Sohn, Y., 1994. *Mapping Low Density Vegetation using Spectral Unmixing in Thematic Mapper Data: Long Valley, Nevada*, Ph.D. Dissertation, University of Utah.

Sohn, Y., and R.M. McCoy, 1997. Mapping Desert Shrub Rangeland Using Spectral Unmixing and Modeling Spectral Mixtures with TM Data, *Photogrammetric Engineering & Remote Sensing*, 63(6):707–716.

Steininger, M.K., 1996. Tropical Secondary Forest Regrowth in the Amazon: age change estimation with Thematic Mapper Data, *International Journal of Remote Sensing*, 17(1):9–27.

Strang, G., 1980. *Linear Algebra and Its Application, Second Edition*, Academic Press, New York.

Villanueva, M.E., 1993. *Crisis henequenera, reconversión económica y movimientos campesinos en Yucatán 1983–1992*, Maldonado editores, Mérida, Yucatan, Mexico.

(Received 03 June 1997; accepted 18 August 1998; revised 27 October 1998)